Inorg. Chem. **2007**, *46*, 4979–4988

Dinuclear Ru^{II}PHEHAT and -TPAC Complexes: Effects of the Second Ru^{II} Center on Their Spectroelectrochemical Properties

Benjamin Elias, Leslie Herman, Cécile Moucheron, and Andrée Kirsch-De Mesmaeker*

Service de Chimie Organique et Photochimie, CP 160/08, Université Libre de Bruxelles, 50 Avenue F. D. Roosevelt, B-1050 Bruxelles, Belgium

Received February 6, 2007

Four novel dinuclear Ru^{II} compounds and, for comparison purposes, two corresponding mononuclear complexes containing the PHEHAT or TPAC ligand (PHEHAT = 1,10-phenanthrolino[5,6-*b*]-1,4,5,8,9,12-hexaazatriphenylene and TPAC = tetrapyrido[3,2-*a*:2′,3′-*c*:3″,2″-*h*:2‴,3‴-*j*]acridine) have been synthesized and characterized. Conclusions on the effects of dinucleation of these two bridging ligands can be drawn only for the compounds for which the results demonstrate that the bridging ligand is involved in the first electrochemical reduction and lowest emission energy. The behavior of these complexes, which is not always predictable, is discussed, and the differences are highlighted in this work. Interestingly, all of the compounds are luminescent except one dinuclear species, $[(phen)_2Ru\text{-}\mu\text{-PHEHAT-}Ru(TAP)_2]^{4+}$, which does not luminesce in MeCN and BuCN at room temperature.

Introduction

The need for new building blocks for the construction of supramolecular entities has become nowadays one of the major targets of several research teams.[1−3] For example, organized polynuclear entities have been prepared for the design of antenna systems to harvest solar energy.[4,5] Organized species have also been studied in single-molecule imaging.[6,7] In order to build these large supramolecular species from coordination complexes, bridging ligands are needed to connect the metallic ion centers. Different types of organic connectors have been used, particularly planar organic ligands.[8−10]

In connection with this research area, we had prepared metallic Ru^{II} multinuclear complexes with building blocks assembled by the PHEHAT bridging ligand (PHEHAT = 1,10-phenanthrolino[5,6-*b*]-1,4,5,8,9,12-hexaazatriphenylene).[11] This heptacyclic ligand is constituted of two motifs: a phenanthroline (phen) and a hexaazatriphenylene (HAT) motif (Figure 1). We had shown that such a ligand induces a direction for the energy-transfer processes inside the corresponding multinuclear Ru^{II} complexes.[12] Another heptacyclic planar bridging ligand, TPAC (tetrapyrido[3,2-*a*:2′,3′-*c*:3″,2″-*h*:2‴,3‴-*j*]acridine; Figure 1), had also been prepared and tested for the connection of two metallic Ru^{II} centers.[13] Despite their similar geometry, the PHEHAT and TPAC ligands have an important structural difference; i.e., PHEHAT has a phenazine as its central motif, whereas TPAC has an acridine motif in the core of the ligand (Figure 1).

The goal of the present work is to investigate the possible different effects of the addition of a second Ru^{II} ion to mononuclear PHEHAT and TPAC complexes, on the electrochemical and photopysical properties of the corresponding dinuclear species. Such a comparison is especially interesting because it was shown that the mononuclear entity

* To whom correspondence should be addressed. E-mail: akirsch@ulb.ac.be.

(1) De Cola, L.; Belser, P. *Coord. Chem. Rev.* **1998**, *177*, 301.
(2) Thébault, F.; Barnett, S. A.; Blake, A. J.; Wilson, C.; Champness, N. R.; Schröder, M. *Inorg. Chem.* **2006**, *45*, 6179.
(3) Polson, M.; Loiseau, F.; Campagna, S.; Hanan, G. S. *Chem. Commun.* **2006**, *12*, 1301.
(4) Balzani, V. *Photochem. Photobiol. Sci.* **2003**, *2*, 459.
(5) Li, W.-S.; Kim, K. S.; Jiang, D.-L.; Tanaka, H.; Kawai, T.; Kwon, J. H.; Kim, D.; Aida, T. *J. Am. Chem. Soc.* **2006**, *128*, 10527.
(6) Ruben, M.; Lehn, J.-M.; Müller, P. *Chem. Soc. Rev.* **2006**, *35*, 1056.
(7) Latterini, L.; Pourtois, G.; Moucheron, C.; Lazzaroni, R.; Brédas, J.-L.; Kirsch-De Mesmaeker, A.; De Schryver, F. C. *Chem.—Eur. J.* **2000**, *6*, 1331.
(8) Kirk, W. P.; Wouters, K. L.; Basit, N. A.; MacDonnell, F. M.; Tao, M.; Clark, K. P. *Physica E* **2003**, *19*, 126.
(9) Patra, S.; Sarkar, B.; Ghumaan, S.; Fiedler, J.; Kaim, W.; Lahiri, G. K. *Dalton Trans.* **2004**, 754.
(10) Serroni, S.; Campagna, S.; Puntoriero, F.; Loiseau, F.; Ricevuto, V.; Passalacqua, R.; Galletta, M. *C. R. Chimie* **2003**, *6*, 883.
(11) Moucheron, C.; Kirsch-De Mesmaeker, A.; Choua, S. *Inorg. Chem.* **1997**, *36*, 584.
(12) Leveque, J.; Elias, B.; Moucheron, C.; Kirsch-De Mesmaeker, A. *Inorg. Chem.* **2005**, *44*, 393.
(13) Demeunynck, M.; Moucheron, C.; Kirsch-De Mesmaeker, A. *Tetrahedron Lett.* **2002**, *43*, 261.

10.1021/ic070224j CCC: $37.00
Published on Web 05/09/2007

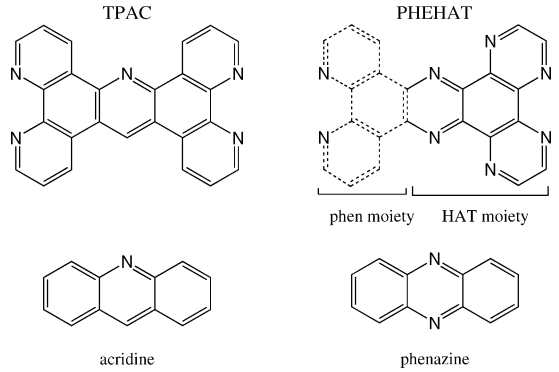

Figure 1. Structure of the PHEHAT and TPAC bridging ligands compared to an acridine moiety and a phenazine moiety.

$[(phen)_2Ru\text{-}PHEHAT]^{2+}$ exhibits a particular behavior.[14] Thus, this study should allow one to highlight the effect of the supplementary heterocyclic N atoms in the PHEHAT ligand as compared to the TPAC ligand. Therefore, for comparison, we had to prepare new mono- and dinuclear Ru^{II} complexes in addition to a list of other compounds already known.

In the present work, we thus present the synthesis, characterization, and electrochemical and photophysical properties of six new mono- and dinuclear complexes based on the PHEHAT and TPAC ligands (Figure 2). Conclusions concerning the specific properties of the PHEHAT and TPAC bridging ligands are presented.

Experimental Section

Instrumentation. ^1H NMR (300 MHz) spectra were obtained on a Bruker Avance-300 instrument. The chemical shifts were measured versus the solvent as the internal standard.

The electrospray mass spectra (ESMS) were obtained with a VG-BIO-QUAD spectrometer. Absorption spectra were recorded on a Perkin-Elmer Lambda UV/vis spectrophotometer. The molar absorption coefficients were determined by weight and absorption measurements.

Emission spectra were recorded with a Shimadzu RF-5001 PC spectrometer equipped with a Hamamatsu R-928 photomultiplier tube and with a 250-W Xe lamp as the excitation source. Measurements were made with complex solutions of 1×10^{-5} mol dm^{-3}. The spectra were corrected for the instrument response except for the measurements at 77 K.

The luminescence lifetimes at room temperature were measured by single photon counting with an Edinburgh Instruments FL900 spectrometer (Edinburgh, U.K.) equipped with a N_2-filled discharge lamp and a Peltier-cooled Hamamatsu R955s photomultiplier tube. The emission decays were analyzed with nonlinear least-squares regressions using Marquardt algorithms (Edinburgh Instruments software, version 3.0).

The luminescence lifetimes as a function of the temperature were measured with a modified Applied Photophysics laser kinetic spectrometer by exciting the samples at 355 nm with a Nd:YAG pulsed laser (Continuum NY 61-10). The emission decays were detected with a R-928 Hamamatsu photomultiplier tube whose ouput was applied to a digital oscilloscope (Hewlett-Packard HP 54200A) interfaced to a Hewlett-Packard HP 9816 S computer. Signals were averaged over 16 shots and corrected for the baseline. Kinetic analyses of the decays were achieved by using Origin 6.0 or Kaleidagraph software.

The experiments as a function of the temperature were carried out using an Oxford Instruments DN 1704 nitrogen cryostat controlled by an Oxford Intelligent Temperature Controller (ITC4) instrument. For the investigated temperature range, the solvent was a liquid.

Cyclic voltammetry was performed in a one-compartment cell, using a glassy carbon disk working electrode (approximate area = 0.03 cm^2), a platinum counterelectrode, and a saturated calomel electrode (SCE) as the reference electrode (Perkin-Elmer Instruments). The potential applied to the working electrode was controlled by an Autolab Potentiostat 100 (Eco Chemie). Scan rates from 100 to 200 mV s^{-1} between -1.8 and $+2.2$ V vs SCE were used. The cyclic voltammograms were recorded with acetonitrile solutions (Acros; acetonitrile for high-performance liquid chromatography, HPLC) and distilled twice over P_2O_5 and once over CaH_2. The concentration of the complexes was 5×10^{-4} mol L^{-1}, with 0.1 mol L^{-1} tetrabutylammonium perchlorate as the supporting electrolyte. Before each measurement, the samples were purged with Ar.

Materials and Methods. $[Ru(phen)_2Cl_2]$,[15] $[Ru(TAP)_2Cl_2]$[16] (TAP = 1,4,5,8-tetraazaphenanthrene), $[(phen)_2Ru\text{-}PHEHAT]^{2+}$,[11] $[(TAP)_2Ru\text{-}PHEHAT]^{2+}$,[17] 5-amino-1,10-phenanthroline,[13] and TPAC[13] were prepared according to procedures described in the literature. All of the solvents and reagents for the syntheses were at least of reagent grade and were used without further purification. All of the solvents for the spectroscopic measurements were of spectroscopic grade. All of the reaction mixtures were protected from direct light during the synthesis to prevent photochemical degradation.

Synthetic Procedures and Characterization. After synthesis and purification (see the description below), the compounds were characterized by ^1H NMR spectroscopy at 300 MHz in CD_3CN. The numbering of the different protons is shown in Figure 2. Protons *X* belonging to phen ligands are labeled "P^X", those belonging to TAP ligands are named "T^X", and those belonging to TPAC and PHEHAT bridging ligands are labeled with Latin italic and Greek letters, respectively. For each complex, the chemical shift (ppm), integration, multiplicity (abbreviations: d = doublet, dd = doublet of doublets), attribution, and coupling constant (*J*, Hz) are reported below. All of the multiplicities and coupling constants could not be determined because of the superposition of several signals and/or the lack of fine resolution for some peaks in the spectra.

For the sake of clarity, the following abbreviations for the different complexes will be used throughout the paper: **T-PHEHAT-p** for $[(TAP)_2Ru\text{-}\mu\text{-}PHEHAT\text{-}Ru(phen)_2]^{4+}$, **p-PHEHAT-T** for $[(phen)_2Ru\text{-}\mu\text{-}PHEHAT\text{-}Ru(TAP)_2]^{4+}$, **p-TPAC-p** for $[(phen)_2Ru\text{-}\mu\text{-}TPAC\text{-}Ru(phen)_2]^{4+}$, **T-TPAC-T** for $[(TAP)_2Ru\text{-}\mu\text{-}TPAC\text{-}Ru(TAP)_2]^{4+}$, **p-TPAC** for $[(phen)_2Ru\text{-}TPAC]^{2+}$, and **T-TPAC** for $[(TAP)_2Ru\text{-}TPAC]^{2+}$.

(a) Dinuclear PHEHAT Complexes. The synthetic strategies used for each dinuclear PHEHAT complex are similar; nevertheless, the reaction times and purification procedures are different.

(1) $[(TAP)_2Ru\text{-}\mu\text{-}PHEHAT\text{-}Ru(phen)_2]^{4+}$ (T-PHEHAT-p). A solution of $[Ru(phen)_2Cl_2]$ (12 mg, 0.023 mmol) and HPLC-purified $[(TAP)_2Ru\text{-}PHEHAT]^{2+}$ (21 mg, 0.019 mmol) in 4 mL of ethylene

(14) Boisdenghien, A.; Moucheron, C.; Kirsch-De Mesmaeker, A. *Inorg. Chem.* **2005**, *44*, 7678.

(15) Sullivan, B. P.; Salmon, D. J.; Meyer, T. J. *Inorg. Chem.* **1978**, *17*, 3334.

(16) Masschelein, A.; Jacquet, L.; Kirsch-De Mesmaeker, A.; Nasielski, J. *Inorg. Chem.* **1990**, *29*, 855.

(17) Moucheron, C.; Kirsch-De Mesmaeker, A. *J. Phys. Org. Chem.* **1998**, *11*, 577.

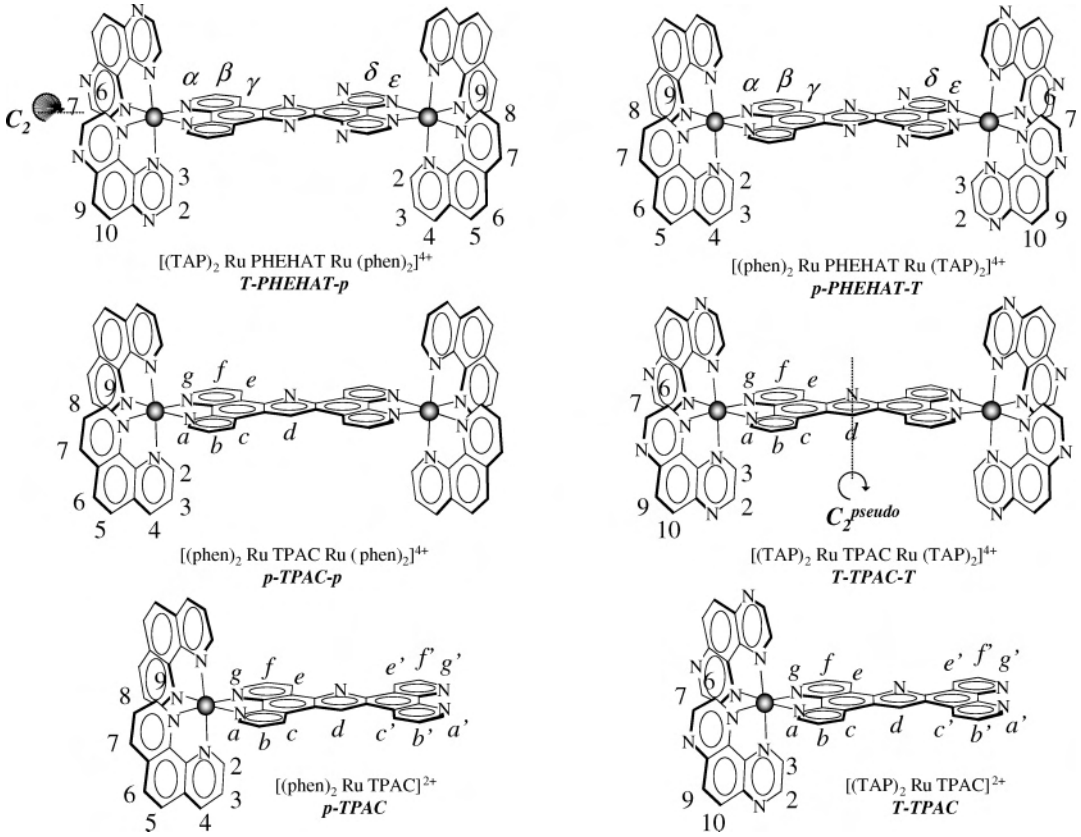

Figure 2. Structure of the novel mono- and dinuclear TPAC and PHEHAT complexes and numbering of the different protons. The symmetry axis is shown in complex $[(TAP)_2Ru\text{-}\mu\text{-}PHEHAT\text{-}Ru(phen)_2]^{4+}$ (**T-PHEHAT-p**) and $[(TAP)_2Ru\text{-}\mu\text{-}TPAC\text{-}Ru(TAP)_2]^{4+}$ (**T-TPAC-T**).

glycol was heated at 150 °C for 120 min. After cooling to room temperature, the addition of water and NH_4PF_6 to the medium yielded a brown-reddish precipitate. The suspension was then centrifuged, and the crude product was washed several times with water and EtOH and finally dried with ether. Preparative layer chromatography on silica, with $CH_3CN-H_2O-NH_4Cl$ saturated in water [4:4:1 (v/v/v)] as the eluent, allowed the purification of **T-PHEHAT-p** (yield = 48%).

^{1}H NMR (CD_3CN), δ/ppm: 7.68 (2H, P^3 and P^8), 7.96 (1H, dd, β, $J_{\beta,\alpha} = 5.5$ Hz), 8.00 (1H, d, P^9, $J_{9,8} = 4.7$ Hz), 8.25 (2H, T^6 and P^2), 8.30 (4H, T^3, P^5, P^6, and α), 8.37 (1H, d, ϵ), 8.63 (2H, AB syst , T^9 and T^{10}), 8.68 (2H, dd, P^4 and P^7, $J_{4,3} = J_{7,8} = 8.3$ Hz, $J_{4,2} = J_{7,9} = 1.2$ Hz), 8.99 (2H, T^2 and T^7), 9.10 (1H, d, δ, $J_{\delta,\epsilon} = 2.9$ Hz), 9.90 (1H, dd, γ, $J_{\gamma,\beta} = 8.5$ Hz, $J_{\gamma,\alpha} = 1.4$ Hz).

ESMS, *m*/*z* (M^{4+} = 1313.3): 328.6 ($[M^{4+}]^{4+}$, 100%; calcd 328.3), 486.4 ($[M^{4+} + PF_6^-]^{3+}$, 45%; calcd 486.1), 802.0 ($[M^{4+} + 2PF_6^-]^{2+}$, 8%; calcd 801.5).

(2) $[(phen)_2Ru\text{-}\mu\text{-}PHEHAT\text{-}Ru(TAP)_2]^{4+}$ (p-PHEHAT-T). A total of 50 mg of $[(phen)_2Ru\text{-}PHEHAT]^{2+}$ (0.044 mmol) and 25 mg of $[Ru(TAP)_2Cl_2]$ (0.047 mmol) were heated at 150 °C under Ar in a mixture of 7 mL of ethylene glycol and 1 mL of *N*,*N*′-dimethylformamide (DMF) for 9 h. After cooling, the addition of an aqueous solution of NH_4PF_6 yielded a brown precipitate, which was washed several times with water and EtOH and finally dried with ether.

The complex was purified by preparative layer chromatography on silica, with $DMF-H_2O-NH_4Cl$ saturated in water [7:1:1 (v/v/v)] as the eluent (yield = 55%).

^{1}H NMR (CD_3CN), δ/ppm: 7.69 (2H, P^3 and P^8), 7.93 (1H, dd, β, $J_{\beta,\alpha} = 5.3$ Hz), 8.07 (1H, d, P^9, $J_{9,8} = 4.9$ Hz), 8.30 (5H, α, P^2, P^5, P^6, and T^6), 8.51 (2H, ϵ and T^3), 8.66 (2H, P^7 and P^4, $J_{4,3} = J_{7,8} = 8.4$ Hz), 8.69 (2H, AB syst, T^9 and T^{10}), 9.06 (2H, d, T^2 and T^7, $J_{2,3} = J_{7,6} = 2.3$ Hz), 9.20 (2H, d, δ, $J_{\delta,\epsilon} = 2.4$ Hz), 9.83 (1H, d, γ, $J_{\gamma,\beta} = 7.9$ Hz).

ESMS, *m*/*z* (M^{4+} = 1313.3): 328.6 ($[M^{4+}]^{4+}$, 100%; calcd 328,3), 486.4 ($[M^{4+} + PF_6^-]^{3+}$, 47%; calcd 486,1), 802.0 ($[M^{4+} + 2PF_6^-]^{2+}$, 6%; calcd 801.5).

(b) Dinuclear TPAC Complexes. In contrast to the dinuclear PHEHAT compounds, the dinuclear TPAC complexes were easily obtained by mixing 1 equiv of free TPAC ligand[13] with 2 equiv of a metallic precursor.

(1) $[(phen)_2Ru\text{-}\mu\text{-}TPAC\text{-}Ru(phen)_2]^{4+}$ (p-TPAC-p) and $[(TAP)_2Ru\text{-}\mu\text{-}TPAC\text{-}Ru(TAP)_2]^{4+}$ (T-TPAC-T). In the case of complex **p-TPAC-p**, 51 mg (0.13 mmol) of readily soluble free TPAC ligand and 162 mg of $[Ru(phen)_2Cl_2]$ (0.30 mmol) were heated in 8 mL of ethylene glycol (130 °C) for 100 min. In the case of **T-TPAC-T**, 50 mg (0.13 mmol) of TPAC was mixed together with 162 mg of $[Ru(TAP)_2Cl_2]$ (0.30 mmol) in 5 mL of ethylene glycol, and the resulting solution was heated at 125 °C for 30 h. After cooling, the addition of water and an excess of NH_4PF_6 produced precipitation in each reaction medium. The resulting orange precipitates were isolated by centrifugation, washed several times with water and EtOH, and finally dried with ether.

Crude products **p-TPAC-p** and **T-TPAC-T** were purified by preparative layer chromatography on silica [eluent for complex **p-TPAC-p**, $CH_3CN-H_2O-NH_4Cl$ saturated in water [4:4:1 (v/v/v), yield = 58%]; eluent for complex **T-TPAC-T**, $DMF-CH_3CN-H_2O-NH_4Cl$ saturated in water [2:1:3:1 (v/v/v/v), yield = 49%].

^{1}H NMR (CD_3CN) for **p-TPAC-p**, δ/ppm: 7.65 (8H, P^3 and P^8), 7.83 (4H, *b* and *f*), 8.05 (4H, d, P^9, $J_{9,8} = 5.2$ Hz), 8.20 (8H, *a*, *g*, and P^2), 8.27 (8H, AB syst, P^5 and P^6), 8.62 (8H, dd, P^4 and P^7, $J_{4,3} = J_{7,8} = 8.3$ Hz, $J_{4,2} = J_{7,9} = 1.1$ Hz), 9.61 (2H, d, *c* or *e*,

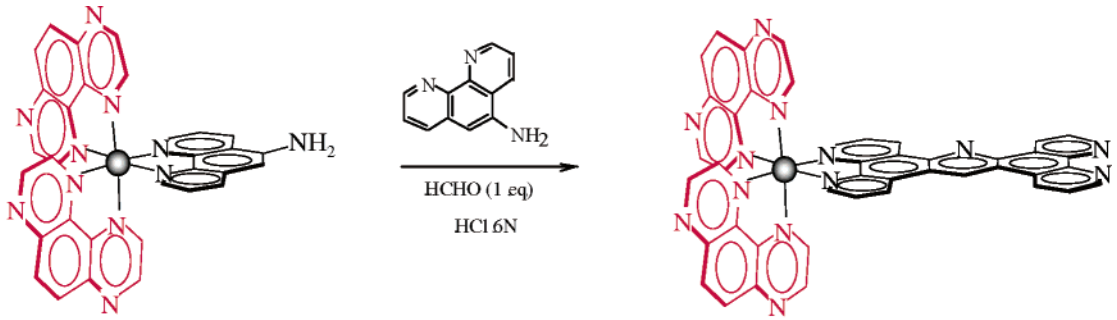

Figure 3. Synthesis of the mononuclear complex $[(TAP)_2Ru\text{-}TPAC]^{2+}$ (**T-TPAC**).

$J_{c,b}$ or $J_{e,f} = 8.3$ Hz), 10.00 (2H, dd, *e* or *c*, $J_{e,f}$ or $J_{c,b} = 8.3$ Hz, $J_{e,g}$ or $J_{c,a} = 1.2$ Hz), 10.51 (1H, s, *d*).

ESMS, *m/z* ($M^{4+} = 1308.4$): 326.9 ($[M^{4+}]^{4+}$, 100%; calcd 327.1), 483.9 ($[M^{4+} + PF_6^-]^{3+}$, 42%; calcd 484.4), 798.6 ($[M^{4+} + 2PF_6^-]^{2+}$, 5%; calcd 799.1).

^{1}H NMR (CD_3CN) for **T-TPAC-T**, δ/ppm: 7.93 (4H, *b* and *f*), 8.24 (8H, *a* and *g*, T^6 or T^3), 8.28 (4H, T^3 or T^6), 8.62 (8H, AB syst, T^9 and T^{10}), 8.96 (8H, T^2 and T^7), 9.70 (2H, d, *c* or *e*, $J_{c,b}$ or $J_{e,f} = 8.4$ Hz), 10.10 (2H, dd, *e* or *c*, $J_{e,f}$ or $J_{c,b} = 8.3$ Hz, $J_{e,g}$ or $J_{c,a} = 1.3$ Hz), 10.66 (1H, s, *d*).

ESMS, *m/z* ($M^{4+} = 1314.3$): 328.9 ($[M^{4+}]^{4+}$, 100%; calcd 328.3), 486.6 ($[M^{4+} + PF_6^-]^{3+}$, 72%; calcd 486.4), 802.6 ($[M^{4+} + 2PF_6^-]^{2+}$, 37%; calcd 802.1).

(c) Mononuclear TPAC Complexes. (1) $[(phen)_2Ru\text{-}TPAC]^{2+}$ (p-TPAC). A total of 25 mg (0.052 mmol) of the TPAC ligand were heated in an 8-mL methanol solution. After complete dissolution of the organic ligand, a solution of 22 mg of $[Ru(phen)_2Cl_2]$ (0.041 mmol) in 1 mL of DMF and 12 mL of MeOH was added dropwise to the reaction medium under vigorous magnetic stirring. The progress of the reaction was followed by absorption spectroscopy and by thin-layer chromatography ($CH_3CN-H_2O-NH_4Cl$ saturated in water [4:4:1 (v/v/v)] as the eluent). When clear changes of the absorption and emission spectra could no longer be recorded (i.e., after 70 min under reflux), the medium was cooled to room temperature. A centrifugation of the reaction medium allowed the elimination of unreacted $[Ru(phen)_2Cl_2]$. The addition of water and an excess of NH_4PF_6 salt in the concentrated medium yielded an orange precipitate, which was washed with water and EtOH and dried with ether. The product was then allowed to crystallize slowly from a saturated CH_3CN solution placed in an ether-saturated closed vessel.

^{1}H NMR (CD_3CN) for **p-TPAC**, δ/ppm: 7.69 (6H, P^3 and P^8, [*b* and *f*], or [*b*′ and *f*′]), 7.83 (2H, [*b*′ and *f*′] or [*b* and *f*]), 8.05 (2H, P^9 or P^2), 8.12 (2H, d, P^2 or P^9, $J_{2,3}$ or $J_{9,8} = 5.0$ Hz), 8.28 (4H, AB syst, P^5 and P^6), 8.48/8.57 (2H, 2d, [*a* and *g*] or [*a*′ and *g*′], $J_{a,b}$ or $J_{a',b'} = J_{g,f}$ or $J_{g',f'} = 5.2$ Hz), 8.62 (6H, P^4 and P^7, [*a*′ and *g*′], or [*a* and *g*]), 9.24/9.39/9.55/9.77 (4H, 4d, *c*, *c*′, *e*, and *e*′, $J_{e,f}$ or $J_{c,b}$ or $J_{e',f'}$ or $J_{c',b'} = 7.9$ Hz/6.9 Hz/8.6 Hz/8.9 Hz), 9.97 (1H, s, *d*).

ESMS, *m/z* ($M^{2+} = 844.9$): 422.5 ($[M^{2+}]^{2+}$, 17%; calcd 422.5), 990.7 ($[M^{2+} + PF_6^-]^+$, 100%; calcd 989.9).

(2) $[(TAP)_2Ru\text{-}TPAC]^{2+}$ (T-TPAC). Whereas no particular problems arose from the synthesis of the mononuclear complex **p-TPAC**, the chelation of $[Ru(TAP)_2Cl_2]$ on free TPAC ligand was unsuccessful. For this reason, complex **T-TPAC** was synthesized according to a different synthetic route. The precursor $[(TAP)_2Ru(5\text{-}NH_2\text{-}phen)]^{2+}$ was first prepared by condensation of $[Ru(TAP)_2Cl_2]$ with 1 equiv of 5-NH_2-phen (5-NH_2-phen = 5-amino-1,10-phenanthroline). Complex **T-TPAC** was obtained afterward by reacting 1 equiv of the monometallic precursor $[(TAP)_2Ru(5\text{-}NH_2\text{-}phen)]^{2+}$ with 1 equiv of 5-NH_2-phen in the presence of *p*-formaldehyde in a 6 N HCl aqueous solution (Figure 3). Thus, 53 mg (0.056 mmol) of $[(TAP)_2Ru(5\text{-}NH_2\text{-}phen)]^{2+}$ and 14 mg (0.072 mmol) of 5-NH_2-phen were added in 5 mL of a 6 N HCl aqueous solution in the presence of 2.3 mg (0.076 mmol) of *p*-formaldehyde. The medium was heated to 90 °C for 8 days under Ar. After neutralization of the reaction medium, the crude product was precipitated from the neutral solution by the addition of small amounts of NH_4PF_6 salt. The brown precipitate was washed several times with water and EtOH, dried with ether, and finally purified by preparative layer chromatography on silica, with formic acid−H_2O-CH_3CN [1:4:4 (v/v/v)] as the eluent.

^{1}H NMR (CD_3CN) for **T-TPAC**, δ/ppm: 7.91 (2H, [*b* and *f*] or [*b*′ and *f*′]), 8.11 (2H, [*b*′ and *f*′] or [*b* and *f*]), 8.26 (6H, [*a* and *g*] or [*a*′ and *g*′], T^3 and T^6), 8.54 (2H, [*a*′ and *g*′] or [*a* and *g*]), 8.63 (4H, AB syst, T^9 and T^{10}), 8.98 (4H, T^2 and T^7), 9.69/9.87/10.12/10.33 (4H, 4d, *c*, *c*′, *e*, and *e*′, $J_{e,f}$ or $J_{c,b}$ or $J_{e',f'}$ or $J_{c',b'} = 8.0$ Hz/7.3 Hz/8.5 Hz/7.7 Hz), 10.54 (1H, s, *d*).

ESMS, *m/z* ($M^{2+} = 848.8$): 424.4 ($[M^{2+}]^{2+}$, 100%; calcd 424.4), 994.6 ($[M^{2+} + PF_6^-]^+$, 9%; calcd 993.8).

Results

Synthesis. The TPAC complexes, with one or two metal centers (i.e., **p-TPAC, p-TPAC-p**, and **T-TPAC-T**), were simply obtained by reacting one or two $[Ru^{II}L_2Cl_2]$ (L = phen or TAP) precursors onto the extended planar ligand. However, despite our numerous attempts, it was not possible to prepare the mononuclear complex **T-TPAC** using the same procedure. Therefore, we had first to synthesize the dicationic precursor $[(TAP)_2Ru\text{-}5\text{-}NH_2\text{-}phen]^{2+}$, which has allowed afterward the direct formation of the extended planar ligand on the Ru^{II} metallic center (Figure 3).

On the other hand, the poor solubility of the PHEHAT heptacycle compared to the TPAC heptacycle in all of the usual organic solvents has not allowed the synthesis of the dinuclear species according to the procedure described above for the TPAC bridging ligand. Therefore, as previously published,[12] another approach based on (i) the synthesis of a soluble mononuclear precursor (the $[(L)_2Ru\text{-}PHEHAT]^{2+}$, L = TAP or phen) and (ii) the chelation of either $[Ru(phen)_2Cl_2]$ or $[Ru(TAP)_2Cl_2]$ onto this monometallic PHE-

HAT precursor has been chosen for the preparation of complexes **T-PHEHAT-p** and **p-PHEHAT-T**, respectively.

It should be mentioned that both the nonsymmetrical dinuclear TPAC complex (i.e., $[(phen)_2Ru$-μ-TPAC-$Ru(TAP)_2]^{4+}$ prepared from either **p-TPAC** or **T-TPAC**) and the dinuclear PHEHAT complex $[(TAP)_2Ru$-μ-PHEHAT-$Ru(TAP)_2]^{4+}$ have not been obtained up to now in sufficiently high yield and purity for their study.

Characterization. The complexes were characterized by ESMS (see the Experimental Section) and by ^1H NMR spectroscopy with $^1H-^1H$ COSY NMR analyses in deuterated acetonitrile. The chemical shifts and corresponding attributions are gathered in the Experimental Section. In the present case, the ^1H NMR spectra show a complete overlapping of the signals for each diastereoisomer, in contrast to polynuclear complexes built with shorter bridging ligands such as dpp[18] (2,3-bis(2-pyridyl)pyrazine) or HAT.[19] The large distance between the two chiral Ru^{II} centers due to the heptacyclic bridging ligands makes the two parts of the dinuclear species distinctive and independent, as was also reported for complexes with the tpphz (tpphz = tetrapyrido-[3,2-*a*:2′,3′-*c*:3″,2″-*h*:2‴,3‴-*j*]phenazine) or tatpp (tatpp = 9,11,20,22-tetraazatetrapyrido[3,2-*a*:2′,3′-*c*:3″,2″-*l*:2‴,3‴-*n*]-pentacene) bridging ligand.[20,21]

(a) PHEHAT Complexes T-PHEHAT-p and p-PHEHAT-T. The C_2 symmetry in these dinuclear complexes (Figure 2) induces the equivalence of (i) the protons on the PHEHAT ligand by pairs (labeled α, β, γ, δ, and ϵ) and (ii) the terminal phen or TAP ligands called P and T, respectively. Because the protons of the TAP and phen ancillary ligands have distinctive chemical shifts, the signals of both external ligands are well distinguishable. A comparison between the chemical shifts of the mononuclear and corresponding dinuclear species (e.g., $[(TAP)_2Ru$-PHEHAT$]^{2+}$ and **T-PHEHAT-p**) shows that the signals for TAP, phen, or PHEHAT are only slightly affected by the addition of a second metallic unit onto the central bridging ligand, except for the ϵ proton of PHEHAT. The latter one, due to the formation of the dinuclear compound **T-PHEHAT-p** or **p-PHEHAT-T**, undergoes a shielding effect, because it is located above ancillary ligands. This shielding is thus characteristic of the chelation of the HAT motif of the PHEHAT bridging ligand by a second Ru^{II} center. In the same way, a comparison with the mononuclear complex $[PHEHAT$-$Ru(phen)_2]^{2+}$ [14] shows that the α protons of the PHEHAT ligand are shielded by about 0.4 ppm when a second Ru^{II} center is chelated onto the phen moiety of the bridging ligand ($\delta_a = 8.71$ ppm in $[PHEHAT$-$Ru(phen)_2]^{2+}$). Even if both complexes **T-PHEHAT-p** and **p-PHEHAT-T** display quite similar ^1H NMR spectra, a comparison between these two dinuclear species indicates that the protons of the ancillary ligands are always more shielded when they are located above the phen moiety than above the HAT moiety of the PHEHAT bridge, in agreement with previously published conclusions.[12]

(b) TPAC Complexes p-TPAC-p, T-TPAC-T, p-TPAC, and T-TPAC. The dinuclear TPAC complexes also have C_2 symmetry. However, unlike dinuclear PHEHAT complexes, the symmetry axis in **p-TPAC-p** and **T-TPAC-T** passes through the central N of the bridging ligand and splits the dinuclear species into two equivalent "monometallic subunits" (Figure 2). Consequently, the presence of this "pseudo-C_2 symmetry" (because the diastereoisomers cannot be distinguished) should theoretically give rise to 23 distinctive ^1H NMR signals for **p-TPAC-p** (19 for complex **T-TPAC-T**) among the 45 protons present in **p-TPAC-p** (37 for complex **T-TPAC-T**). However, only a few signals are detected. This indicates that, although all of the protons of both ancillary ligands of one Ru^{II} center are chemically different, the same protons in each ancillary ligand are undistinguishable, as indicated by the integration.

In contrast, the mononuclear TPAC complexes **p-TPAC** and **T-TPAC** do not display any symmetry features, as is clearly shown from the analysis of the NMR data. Indeed, the number of signals increases from the dinuclear complex **p-TPAC-p** to the mononuclear complex **p-TPAC**. Interestingly, a slight doubling of the signals is observed for both protons P^2 and P^9, probably because of the anisotropy induced by the asymmetry of the TPAC ligand. Although this effect should also be present in the dinuclear **p-TPAC-p**, it could not be detected in our experimental conditions. Moreover, the protons *a*/*g* and *a*′/*g*′ of the TPAC ligand have almost the same chemical shift, although they are located in different parts of the molecule. The same discussion can be drawn for the mononuclear complex **T-TPAC** and the related dinuclear species **T-TPAC-T**.

It should also be stressed that the signals of the mononuclear compounds **p-TPAC** and **T-TPAC** are very sensitive to the concentration. This effect is the most pronounced for the protons of the TPAC ligand and can be attributed to some π stacking of the TPAC ligand as observed with other ligands.[20,22]

Electrochemistry. The redox potentials of the six novel complexes and reference compounds determined by cyclic voltammetry in dry deoxygenated acetonitrile solutions are gathered in Table 1.

(a) Oxidation. (1) TPAC Complexes. The dinuclear TPAC complexes **p-TPAC-p** and **T-TPAC-T** exhibit one reversible bielectronic oxidation wave at +1.31 and +1.76 V vs SCE, respectively. A comparison with each of the corresponding mononuclear complexes (i.e., **p-TPAC** and **T-TPAC**) shows that the oxidation potentials are approximately the same between the mono- and dinuclear species. The second Ru^{II} ion on the bridging ligand has thus very little influence on these values, which suggests a rather poor electronic interaction between the two metal centers,

(18) Campagna, S.; Denti, G.; Serroni, S.; Juris, A.; Venturi, M.; Ricevuto, V.; Balzani, V. *Chem.—Eur. J.* **1995**, *1*, 211.
(19) Leveque, J.; Moucheron, C.; Kirsch-De Mesmaeker, A.; Loiseau, F.; Serroni, S.; Puntoriero, F.; Campagna, S.; Nierengarten, H.; Van Dorsselaer, A. *Chem. Commun.* **2004**, 878.
(20) Campagna, S.; Serroni, S.; Bodige, S.; MacDonnell, F. M. *Inorg. Chem.* **1999**, *38*, 692.
(21) Konduri, R.; de Tacconi, N. R.; Rajeshwar, K.; MacDonnell, F. M. *J. Am. Chem. Soc.* **2004**, *126*, 11621.
(22) Gut, D.; Goldberg, I.; Kol, M. *Inorg. Chem.* **2003**, *42*, 3483.

Table 1. Electrochemical Data Measured by Cyclic Voltammetry in Acetonitrile versus SCE at Room Temperature, for the Six Novel Complexes and Other Reference Compounds for Comparison Purposes (in Parentheses, the Number of Associated Electrons)

E_{ox} (V vs SCE)			E_{red} (V vs SCE)		
1	**2**	complex	**1**	**2**	**3**
+1.50 (1)	+1.86 (1)	$[(TAP)_2Ru\text{-}\mu\text{-}PHEHAT\text{-}Ru(phen)_2]^{4+}$	−0.57 (1)	−0.79 (1)	
+1.39 (1)	+2.10[a]	$[(phen)_2Ru\text{-}\mu\text{-}PHEHAT\text{-}Ru(TAP)_2]^{4+}$	−0.52 (1)	−0.76 (1)	
+1.34 (1)	+1.55 (1)	$[(phen)_2Ru\text{-}\mu\text{-}PHEHAT\text{-}Ru(phen)_2]^{4+}$ [b]	−0.68 (1)	−1.06 (1)	
+1.80 (1)		$[(TAP)_2Ru\text{-}PHEHAT]^{2+}$ [c]	−0.75		
+1.35 (1)		$[(phen)_2Ru\text{-}PHEHAT]^{2+}$ [d]	−1.00[a]	−1.25	
+1.53 (1)		$[HAT\text{-}Ru(phen)_2]^{2+}$ [e]	−0.86	−1.42	−1.69
+1.56 (1)		$[PHEHAT\text{-}Ru(phen)_2]^{2+}$ [d]	−0.83	−1.21	
+2.03 (1)		$[HAT\text{-}Ru(TAP)_2]^{2+}$ [e]	−0.68	−0.86	−1.08
+1.73 (1)		$[(TAP)_2Ru\text{-}phen]^{2+}$ [f]	−0.83	−1.01	−1.55
+1.27 (1)		$[(phen)_2Ru\text{-}phen]^{2+}$ [g]	−1.35 (1)	−1.52 (1)	
+1.76 (2)		$[(TAP)_2Ru\text{-}\mu\text{-}TPAC\text{-}Ru(TAP)_2]^{4+}$	−0.76 (2)	−0.92 (2)	−1.26 (1)
+1.31 (2)		$[(phen)_2Ru\text{-}\mu\text{-}TPAC\text{-}Ru(phen)_2]^{4+}$	−1.10 (1)	−1.32 (2)	−1.57 (2)
+1.70 (1)		$[(TAP)_2Ru\text{-}TPAC]^{2+}$	−0.81 (1)	−0.97 (1)	
+1.33 (1)		$[(phen)_2Ru\text{-}TPAC]^{2+}$	−1.15 (1)	−1.25 (1)	−1.35 (1)

[a] Poorly resolved. [b] This complex was discussed in the frame of studies of tetranuclear species; see ref 12 for further discussion. [c] From ref 23. [d] From ref 14. [e] From ref 24. [f] From ref 25. [g] From ref 27.

as confirmed by the presence of only one oxidation wave of two electrons. From these data, it can also be concluded that the energy level of the dπ orbital of the TAP-containing complexes, **T-TPAC-T** and **T-TPAC** (+1.76 and +1.70 V vs SCE), is more stabilized than that of the phen-containing complexes **p-TPAC-p** and **p-TPAC** (+1.31 and +1.33 V vs SCE).

(2) PHEHAT Complexes. In contrast to the TPAC complexes, the dinuclear PHEHAT complexes exhibit two oxidation waves of one electron at +1.50 and +1.86 V vs SCE for **T-PHEHAT-p** and at +1.39 and >+2.10 V vs SCE for **p-PHEHAT-T**. A comparison of these values with those of the mononuclear species, thus for **T-PHEHAT-p**, with $[(TAP)_2Ru\text{-}PHEHAT]^{2+}$ [23] (E_{ox} = +1.80 V vs SCE) and with $[HAT\text{-}Ru(phen)_2]^{2+}$ [24] (E_{ox} = +1.53 V vs SCE), indicates that "HAT-Ru(phen)$_2$" is the first moiety to be oxidized. For **p-PHEHAT-T**, a comparison with $[(phen)_2Ru\text{-}PHEHAT]^{2+}$ [14] (E_{ox} = +1.35 V vs SCE) and $[HAT\text{-}Ru(TAP)_2]^{2+}$ [24] (E_{ox} = +2.03 V vs SCE) indicates that "(phen)$_2$Ru-PHEHAT" is the first entity to be oxidized. It is also clear that again the Ru^{II} ions with two TAP ligands (with a high electron-withdrawing power) are less easily oxidized and have thus the most stabilized dπ orbital.

(b) Reduction. (1) TPAC Complexes. The dinuclear TPAC complex **p-TPAC-p** exhibits a first reversible one-electron reduction wave at −1.10 V vs SCE, which cannot correspond to the reduction of a phen ancillary ligand because the first reduction for $[Ru(phen)_3]^{2+}$ occurs at −1.35 V vs SCE. Consequently, the first reduction of **p-TPAC-p** is attributed to the addition of one electron to the TPAC bridging ligand. Only a slight anodic shift has occurred for this first reduction as compared to that of the mononuclear complex **p-TPAC** (−1.15 V vs SCE). This indicates a very small stabilization of the π* orbital localized on the bridging ligand due to the addition of a second metallic unit on the bridging TPAC. The second and third reduction waves of **p-TPAC-p** are attributed to two successive simultaneous additions of two electrons to each phen ancillary ligand located on each side of the TPAC bridging ligand. The reduction patterns for the complexes **T-TPAC-T** and **T-TPAC** are comparable for the first two potentials. According to previously published results,[25] they can be unambiguously attributed to the addition of one electron to each TAP ancillary ligand (two electrons simultaneously added to **T-TPAC-T** and one electron to **T-TPAC**). For these two complexes, the lowest π* orbital involved is thus localized on the TAP ancillary ligand. The third reduction process for complex **T-TPAC-T** could correspond to the reduction of the TPAC ligand.

(2) PHEHAT Complexes. Whereas the measurements of the reduction potentials for all TPAC complexes did not present any particular problem, this was not the case for the dinuclear PHEHAT complexes **T-PHEHAT-p** and **p-PHEHAT-T**. Only the first and second reduction waves could be measured within the potential range of 0 to −1.20 V vs SCE. At more cathodic potentials, a set of poorly resolved and irreversible waves was obtained, probably because of adsorption on the electrode. The two successive reduction processes of one electron (around −0.55 and −0.78 V vs SCE) appear almost at the same potentials for both complexes. As compared to the reduction of $[(phen)_2Ru\text{-}\mu\text{-}PHEHAT\text{-}Ru(phen)_2]^{4+}$, for which the first and second reductions could be assigned to the addition of first and second electrons to the central PHEHAT, the same attribution could be done for **T-PHEHAT-p** and **p-PHEHAT-T**. For these latter complexes, there is a slight anodic shift as compared to that of $[(phen)_2Ru\text{-}\mu\text{-}PHEHAT\text{-}Ru(phen)_2]^{4+}$ because both **T-PHEHAT-p** and **p-PHEHAT-T** contain two TAP ligands with important electron-withdrawing ability, which seem to have approximately the same influence on the reduction potential independently of their site of chelation (on the left or right side). Moreover, even without TAP ligands, the reduction of $[(phen)_2Ru\text{-}\mu\text{-}PHEHAT\text{-}Ru(phen)_2]^{4+}$ on the PHEHAT ligand (−0.68 V vs SCE) is anodically

(23) Debecker, B., unpublished results, Ph.D. Thesis, Université Libre de Bruxelles, Bruxelles, Belgium, Dec 2003.

(24) Jacquet, L.; Kirsch-De Mesmaeker, A. *J. Chem. Soc., Faraday Trans.* **1992**, *88*, 2471.

(25) Ortmans, I.; Elias, B.; Kelly, J. M.; Moucheron C.; Kirsch-De Mesmaeker, A. *Dalton Trans.* **2004**, 668.

Table 2. Absorption Data in Aerated CH_3CN at 298 K for the Six Novel Complexes (in Bold Type) Together with Other Reference Compounds for Comparison Purposes (sh = Shoulder)

complex	λ_{max} absorption, nm ($\epsilon/10^3$ M^{-1} cm^{-1})	
	UV	visible
$[(TAP)_2Ru\text{-}\mu\text{-}PHEHAT\text{-}Ru(phen)_2]^{4+}$	272, 366	410, 446 (24.3), 480^{sh}
$[(phen)_2Ru\text{-}\mu\text{-}PHEHAT\text{-}Ru(TAP)_2]^{4+}$	266, 370	420, 440 (30.1)
$[(phen)_2Ru\text{-}\mu\text{-}PHEHAT\text{-}Ru(phen)_2]^{4+}$ [a]	261, 288^{sh}, 309^{sh}, 330^{sh}, 368	420^{sh}, 444 (28.1), 475^{sh}
$[(TAP)_2Ru\text{-}PHEHAT]^{2+}$ [b]	276, 362	414 (16.3), 450
$[(phen)_2Ru\text{-}PHEHAT]^{2+}$ [c]	264, 278^{sh}, 312^{sh}, 354^{sh}, 370	438
$[HAT\text{-}Ru(phen)_2]^{2+}$ [d]	262	420 (14.4), 480^{sh}
$[PHEHAT\text{-}Ru(phen)_2]^{2+}$ [c]	260, 288^{sh}, 316, 364, 382	428, 478^{sh}
$[HAT\text{-}Ru(TAP)_2]^{2+}$ [d]	202, 229, 272	409, 438
$[(TAP)_2Ru\text{-}phen]^{2+}$ [e]	272	412, 458
$[(phen)_2Ru\text{-}phen]^{2+}$ [f]	262	446 (18)
$[(TAP)_2Ru\text{-}\mu\text{-}TPAC\text{-}Ru(TAP)_2]^{4+}$	279, 317^{sh}	418 (36.1), 460^{sh}
$[(phen)_2Ru\text{-}\mu\text{-}TPAC\text{-}Ru(phen)_2]^{4+}$	263, 280^{sh}, 320^{sh}, 357	418^{sh}, 450 (49.1)
$[(TAP)_2Ru\text{-}TPAC]^{2+}$	203, 231, 279, 319^{sh}	415 (11.9), 462^{sh}
$[(phen)_2Ru\text{-}TPAC]^{2+}$	263, 284, 314^{sh}, 363	415^{sh}, 450 (14.3)

[a] This complex was discussed in the frame of studies of tetranuclear species; see ref 12 for further discussion. [b] From ref 23. [c] From ref 14. [d] From ref 24. [e] From ref 25. [f] From ref 27.

Table 3. Emission Data in an Aerated CH_3CN Solution at 298 K and in a Rigid Matrix of MeOH/EtOH (4:1) at 77 K for the Six Novel Complexes and Reference Compounds for Comparison Purposes

complex	λ_{max} emission, nm		assignment of the luminophore
	298 K, CH_3CN	77 K, MeOH/EtOH (4:1)	
$[(TAP)_2Ru\text{-}\mu\text{-}PHEHAT\text{-}Ru(phen)_2]^{4+}$	701	663	HAT-Ru
$[(phen)_2Ru\text{-}\mu\text{-}PHEHAT\text{-}Ru(TAP)_2]^{4+}$		604	Ru-PHEHAT
$[(phen)_2Ru\text{-}\mu\text{-}PHEHAT\text{-}Ru(phen)_2]^{4+}$ [a]	706	660	HAT-Ru
$[(TAP)_2Ru\text{-}PHEHAT]^{2+}$ [b]	628	588[c]	TAP-Ru
$[(phen)_2Ru\text{-}PHEHAT]^{2+}$ [d]	662	598	Ru-PHEHAT
$[HAT\text{-}Ru(phen)_2]^{2+}$ [d]	694	650	HAT-Ru
$[PHEHAT\text{-}Ru(phen)_2]^{2+}$ [d]	692	663	HAT-Ru
$[HAT\text{-}Ru(TAP)_2]^{2+}$ [e]	595	575	HAT-Ru
$[(TAP)_2Ru\text{-}phen]^{2+}$ [f]	626	590[g]	TAP-Ru
$[(phen)_2Ru\text{-}phen]^{2+}$ [h]	604	566[i]	phen-Ru
$[(TAP)_2Ru\text{-}\mu\text{-}TPAC\text{-}Ru(TAP)_2]^{4+}$	623	592	Ru-TAP
$[(phen)_2Ru\text{-}\mu\text{-}TPAC\text{-}Ru(phen)_2]^{4+}$	612	573	Ru-TPAC
$[(TAP)_2Ru\text{-}TPAC]^{2+}$	624	590	TAP-Ru
$[(phen)_2Ru\text{-}TPAC]^{2+}$	608	570	Ru-TPAC

[a] This complex was discussed in the frame of studies of tetranuclear species; see ref 12 for further discussion. [b] From ref 23. [c] Measured in BuCN (solubility problem in MeOH/EtOH); from ref 23. [d] From ref 14. [e] From ref 24. [f] From ref 25. [g] From ref 28. [h] From ref 27. [i] From ref 24.

shifted as compared to the value of $[(phen)_2Ru\text{-}PHEHAT]^{2+}$ (−1.00 V vs SCE). In conclusion, when a second metal ion is added to the bridging PHEHAT ligand, the reduction data indicate that the π^* orbital centered on the PHEHAT ligand is much more stabilized than the π^* orbital centered on the TPAC ligand.

Absorption and Emission (See Also Figures S1−S3 in the Supporting Information). The absorption data in acetonitrile are collected in Table 2 for the six novel complexes and for reference complexes. Each compound displays several absorption bands in the UV region (ligand-centered transitions) and in the visible region [metal-to-ligand charge-transfer (MLCT) transitions Ru → L, where L = phen, TPAC, PHEHAT, HAT, or TAP]. The absorption of polynuclear species may correspond to the superposition of absorption of each metal-based chromophore.[12,26] Indeed, for **T-PHEHAT-p** and $[(phen)_2Ru\text{-}\mu\text{-}PHEHAT\text{-}Ru(phen)_2]^{4+}$, two components can be distinguished in the visible region (446 and 480 nm and 444 and 475 nm, respectively). The most bathochromic one at 480 or 475 nm could correspond to the $[PHEHAT\text{-}Ru(phen)_2]^{2+}$ species (Table 2). For **p-PHEHAT-T**, the absorptions of each metallic subunit appears approximately at the same wavelength and hence are not well distinguishable. Because dinuclear TPAC complexes **p-TPAC-p** and **T-TPAC-T** are symmetrical, the two metal-based chromophores are equivalent. The most bathochromic transitions in these complexes correspond to a charge transfer toward the lowest π^* orbital, thus for **p-TPAC-p**, according to the reduction data, to the TPAC ligand and for **T-TPAC-T** to the TAP ligand. Moreover, a comparison of the absorption data for these two complexes with those of their related mononuclear compounds (**p-TPAC** or **T-TPAC**) does not indicate any influence of the second metallic moiety.

The luminescence spectra recorded in acetonitrile at room temperature show one typical MLCT emission (with one λ_{max}), originating from one luminophore except for **p-PHEHAT-T**. The data along with those for reference complexes are collected in Table 3. Each emission maximum is independent of the excitation wavelength, which indicates that for the asymmetrical dinuclear complexes intramolecular energy transfer to the lowest emitter is efficient.

(26) Balzani, V.; Campagna, S.; Denti, G.; Juris, A.; Serroni, S.; Venturi, M. *Acc. Chem. Res.* **1998**, *31*, 26.

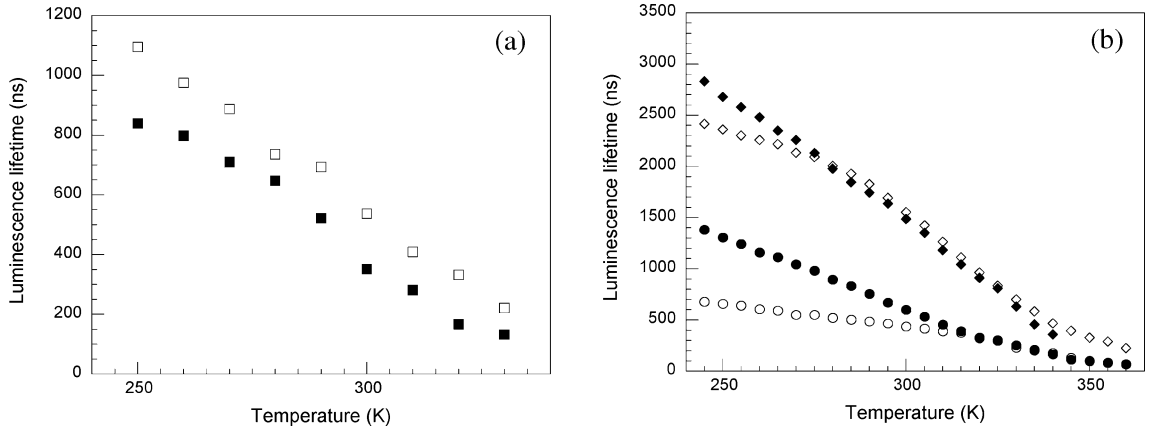

Figure 4. Luminescence lifetimes as a function of the temperature for (a) the PHEHAT complexes **p-PHEHAT-p** (filled squares) and **T-PHEHAT-p** (empty squares) and for (b) the TPAC complexes **p-TPAC** (empty circles), **p-TPAC-p** (filled circles), **T-TPAC** (empty diamonds), and **T-TPAC-T** (filled diamonds). All of the lifetimes are measured in an Ar-purged BuCN solution at the emission maximum of each complex.

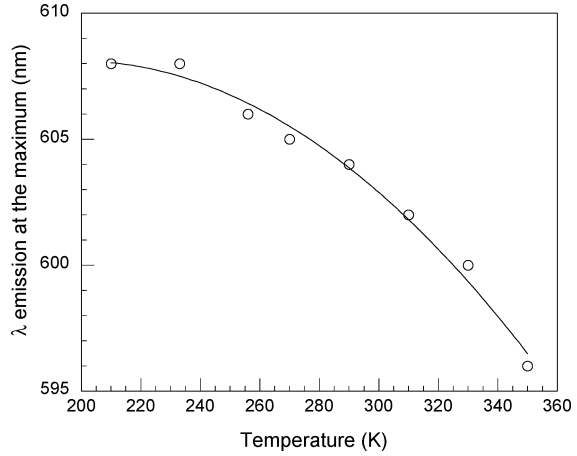

Figure 5. Evolution of the emission maximum of complex **p-TPAC** in BuCN as a function of the temperature.

The complexes **T-PHEHAT-p** and $[(phen)_2Ru\text{-}\mu\text{-}PHEHAT\text{-}Ru(phen)_2]^{4+}$ exhibit at room temperature and 77 K a luminescence close to that of one monometallic subunit, i.e., $[PHEHAT\text{-}Ru(phen)_2]^{2+}$ or $[HAT\text{-}Ru(phen)_2]^{2+}$. The luminescence lifetimes as a function of the temperature in BuCN for these two dinuclear complexes increase monotonically with decreasing temperature (Figure 4a), and no shift of the emission maximum was detected for both complexes in the same temperature range. In contrast, the dinuclear species **p-PHEHAT-T** does not emit (Table 3) at room temperature or in the 360−240 temperature range in BuCN or MeCN. However, an emission is observed at 604 nm in a matrix at 77 K, which would suggest that it originates from the "$(phen)_2$Ru-PHEHAT" moiety.

The dinuclear TPAC complexes show very little differences in emission between the mononuclear and related dinuclear species at room temperature or in a rigid matrix at 77 K. Figure 4b shows the luminescence lifetimes as a function of the temperature for the four TPAC complexes. None of them exhibits a dependence of the emission maximum with decreasing temperature, except **p-TPAC** (Figure 5).

Discussion

TPAC Complexes T-TPAC and T-TPAC-T. For **T-TPAC-T**, the effect of dinucleation cannot be studied. Indeed, the electrochemical and spectroscopic data indicate clearly that the TAP π^* orbital is involved in the lowest transitions of these TAP complexes, without contribution of the TPAC ligand. Moreover, as measured for the other TAP complexes, the luminescence lifetimes for both **T-TPAC** and **T-TPAC-T** increase monotonically with decreasing temperatures (Figure 4b). In a solvent matrix at 77 K, the emission maximum is also the same for both complexes and for the reference mononuclear complex $[(TAP)_2Ru\text{-}phen]^{2+}$. This indicates that the luminophore typically corresponds to a Ru−TAP MLCT transition and the electrochemical and spectroscopic data can be correlated for these two complexes.

In contrast, for the other dinuclear species with TPAC and PHEHAT, the influence of the dinucleation on the spectroelectrochemical properties can be examined. Indeed, in each case, the lowest MLCT transitions involve the bridging ligand (vide supra). We will first examine the case of the three dinuclear PHEHAT complexes by comparison with their related mononuclear species.

Dinuclear PHEHAT Complexes. It was shown previously that the emission of the mononuclear complex $[(phen)_2Ru\text{-}PHEHAT]^{2+}$ exhibits a particular behavior. The emission lifetimes as a function of the temperature in BuCN show the presence of a maximum around 320 K.[14] This means that decreasing the temperature from 320 to 240 K induces a continuous shortening of the lifetime. From these studies and measurements of emission spectra as a function of the temperature, we had demonstrated that at least three states participate in the excited-state deactivation processes: a higher energy state (bright state 1, Figure 6) with the electron localized on the phen motif of PHEHAT, a lower energy state (bright state 2, Figure 6) with the electron more delocalized on PHEHAT, and a nonluminescent state (dark state, Figure 6) still lower in energy. In contrast, $[PHEHAT\text{-}Ru(phen)_2]^{2+}$ (i.e., the mononuclear compound in which the metallic Ru^{II} center is chelated to the HAT part of PHEHAT) has only one emitter similar to that of $[HAT\text{-}Ru(phen)_2]^{2+}$.

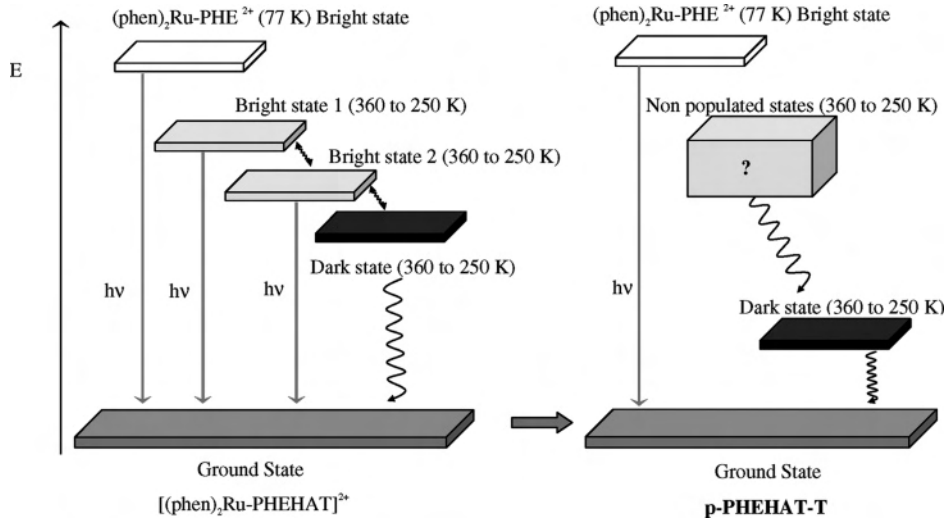

Figure 6. Schematic representation of an energy level diagram that can be proposed from the photophysical study at 77 K in a solvent matrix [bright state 1, luminophore = Ru-phen part of PHEHAT (abbreviated as $(phen)_2$Ru-PHE)] and in BuCN from 360 to 250 K for the complexes $[(phen)_2Ru\text{-}PHEHAT]^{2+}$ (adapted from ref 14, on the left) and **p-PHEHAT-T** (on the right). In this latter case, the unknown states labeled with a question mark are not populated at 360−250 K because they would deactivate quickly to the dark state, lower in energy than that of $[(phen)_2Ru\text{-}PHEHAT]^{2+}$; see the text.

Thus, the properties of the mononuclear PHEHAT/HATPHE complexes clearly depend on the chelation site.[14] These striking results had thus motivated us to investigate the behavior of the new dinuclear PHEHAT species.

For $[(phen)_2Ru\text{-}\mu\text{-}PHEHAT\text{-}Ru(phen)_2]^{4+}$, the emission (λ_{max}^{em} = 706 nm) corresponds to that of $[HAT\text{-}Ru(phen)_2]^{2+}$ (λ_{max}^{em} = 694 nm) or $[PHEHAT\text{-}Ru(phen)_2]^{2+}$ (λ_{max}^{em} = 692 nm), which indicates that the lowest ^{3}MLCT state originates from a Ru−HAT (HAT part of PHEHAT) transition. $[(phen)_2Ru\text{-}\mu\text{-}PHEHAT\text{-}Ru(phen)_2]^{4+}$ exhibits also a "normal" monotonic increase of luminescence lifetimes in BuCN for decreasing temperatures (Figure 4a), in agreement with a MLCT Ru−HAT emitting state. At 77 K, the emission of the dinuclear species corresponds also to a Ru-HAT luminophore ($\lambda_{max,77K}^{em}$ = 660 nm) in comparison with the mononuclear $[HAT\text{-}Ru(phen)_2]^{2+}$ ($\lambda_{max,77K}^{em}$ = 650 nm) or $[PHEHAT\text{-}Ru(phen)_2]^{2+}$ ($\lambda_{max,77K}^{em}$ = 663 nm). However, in disagreement with this spectroscopic behavior, the electrochemistry in reduction does not correspond either to the reduction of a $[HAT\text{-}Ru(phen)_2]^{2+}$ species or to that of a $[PHEHAT\text{-}Ru(phen)_2]^{2+}$ species (Table 1). The reduction potential has a less negative value (E^{red} = −0.68 V vs SCE), which should correspond to the reduction of the PHEHAT ligand, whose π^* orbital is much more stabilized compared to that of the mononuclear complexes. Therefore, in the case of $[(phen)_2Ru\text{-}\mu\text{-}PHEHAT\text{-}Ru(phen)_2]^{4+}$, the electrochemical and spectroscopic data cannot be correlated.

As mentioned above, the synthetic route used for the PHEHAT complexes has allowed the introduction of a "Ru-$(TAP)_2$" species selectively either at the phen motif (in the case of **T-PHEHAT-p**) or at the HAT motif (in the case of **p-PHEHAT-T**) of the PHEHAT bridging ligand. From the present results, we have seen that the site of introduction of the TAP ligands in the dinuclear PHEHAT complexes does not induce a difference between the reduction potentials of the PHEHAT ligand in **T-PHEHAT-p** and **p-PHEHAT-T**. This contrasts with the spectroscopic properties. As inferred from the absorption and emission data (room temperature and 77 K), the properties of **T-PHEHAT-p** are governed by the "HAT-Ru$(phen)_2$" or "PHEHAT-Ru$(phen)_2$" moiety. In agreement with this, the luminescence lifetimes as a function of the temperature for **T-PHEHAT-p** do not show the presence of any maximum, as for the mononuclear $[HAT\text{-}Ru(phen)_2]^{2+}$ or $[PHEHAT\text{-}Ru(phen)_2]^{2+}$ complex. In contrast, **p-PHEHAT-T** is not luminescent in BuCN or MeCN in the whole investigated temperature range from 360 to 250 K, whereas in a rigid matrix at 77 K, the luminescence corresponds to that of $[(phen)_2Ru\text{-}PHEHAT]^{2+}$. These observations would be in agreement with an energy transfer to the $[(phen)_2Ru\text{-}PHEHAT]^{2+}$ part. Indeed as explained above, the mononuclear $[(phen)_2Ru\text{-}PHEHAT]^{2+}$ complex has a nonemissive dark state whose population increases with decreasing temperatures.[14] Thus, the absence of luminescence for **p-PHEHAT-T** would suggest that such a dark state would also exist for this complex. Moreover, because of the second nucleation of the PHEHAT bridging ligand by a Ru-$(TAP)_2^{2+}$ entity, this state would be more stabilized compared to that of the mononuclear complex (Figure 6), so that **p-PHEHAT-T** would be nonluminescent from room temperature until 250 K. This nonluminescent species would correspond to a charge-separated state in which the back-electron-transfer would take place in a time domain faster than the lifetime of a ^{3}MLCT state; this fast back-electron-transfer would be facilitated, as postulated by Schanze and co-workers,[29] by a rapid triplet−singlet spin-conversion process in a charge-separated state. In contrast, as explained for the mononuclear complex $[(phen)_2Ru\text{-}PHEHAT]^{2+}$, the emission of **p-PHEHAT-T** is restored at 77 K[14] because of the absence of relaxation of the solvent around the MLCT

(27) Barigelletti, F.; Juris, A.; Balzani, V.; Belser, P.; von Zelewsky, A. *Inorg. Chem.* **1987**, *26*, 4115.
(28) Lecomte, J.-P.; Kirsch-De Mesmaeker, A.; Demeunynck, M.; Lhomme, J. *J. Chem. Soc., Faraday Trans.* **1993**, *89*, 3261.
(29) Schanze, K. S.; Walters, K. A. *Organic and Inorganic Photochemistry*; Marcel Dekker: New York, 1998; pp 75−127.

excited state, when the excited electron remains closer to the Ru center of the "$(phen)_2$Ru-PHEHAT" part.

TPAC Complexes p-TPAC-p and p-TPAC. As mentioned above, the electrochemical and spectroscopic data indicate that for these two TPAC complexes the lowest MLCT transition is a Ru−TPAC transition and there is very little influence of dinucleation on these properties. The oxidation of the dinuclear **p-TPAC-p** corresponds indeed to a bielectronic wave, with a potential close to that of the mononuclear entity. Again, for **p-TPAC** and **p-TPAC-p**, the luminescence lifetimes as a function of the temperature (Figure 4b) clearly do not display any maximum in the curve (unlike $[(phen)_2$Ru-PHEHAT$]^{2+}$) in the examined temperature range for which the solvent is still a liquid. However, for **p-TPAC**, the increase of the lifetime at lower temperatures (Figure 4b) is different from that of the dinuclear species **p-TPAC-p**. Moreover, Figure 5 shows variation of the emission maximum of **p-TPAC** with decreasing temperatures. Although the shift is rather small within the investigated temperature range, this was not observed for the other complexes. This behavior could be due to the presence of two emitting states differently populated with temperature. Because the lowest transition corresponds to a Ru−TPAC MLCT transition, one can speculate that, after excitation, the electron (i) is located on the phen moiety of the TPAC ligand (i.e., close to the metallic center) and (ii) at lower temperatures moves further toward the central acridine moiety of the ligand. Two luminescent excited states could thus participate in the deactivation and lead to a nonmonotonous evolution of the luminescence lifetimes with decreasing temperatures.

Conclusions

The free soluble TPAC ligand has allowed the direct chelation of one or two identical metallic center(s) to the bridging ligand, leading to mono- or dinuclear symmetrical complex(es). Because the PHEHAT ligand is not soluble in the usual solvents, the preparation of dinuclear PHEHAT complexes has been performed by the chelation of a dichloro metallic complex $[Ru(L)_2Cl_2]$ to a soluble monometallic precursor $[(L)_2$Ru-PHEHAT$]^{2+}$ (L = phen or TAP). This synthetic route offers the possibility of preparing nonsymmetrical dinuclear species.

From examination of the electrochemical and spectroscopic properties, some clear conclusions can be drawn. Obviously, the effect of dinucleation of the PHEHAT or TPAC complexes can be highlighted only when the bridging ligand is involved in the first electrochemical reduction and lowest spectroscopic transition. The addition of a second Ru ion has a different effect on the properties of the TPAC complexes compared to the PHEHAT dinuclear complexes. For the TPAC complexes, there is almost no effect on the electrochemistry or spectroscopy. However, as is inferred from the spectroscopic data, it seems that two luminescent states would participate in the deactivation of the **p-TPAC** excited states. For the PHEHAT dinuclear compounds, the reduction potentials of the PHEHAT bridging ligand are affected by the addition of a second Ru cation and depend on the ancillary ligands. This indicates that the presence of supplementary N atoms in PHEHAT compared to TPAC would favor "electronic communication" between the two metal centers. However, from the spectroscopic behavior of **T-PHEHAT-p** or $[(phen)_2$Ru-μ-PHEHAT-Ru$(phen)_2]^{4+}$, only one part of the bridging ligand would control the photophysics (the HAT motif). Interestingly, when the lowest MLCT transition originates from the "$(phen)_2$Ru-PHEHAT" subunit (in the case of **p-PHEHAT-T**), no luminescence is observed in MeCN or BuCN. On the basis of the behavior of the mononuclear complex $[(phen)_2$Ru-PHEHAT$]^{2+}$,[14] we propose that only a "dark state" would be populated at room temperature in **p-PHEHAT-T**.

In conclusion, the systematic study of the different dinuclear PHEHAT and TPAC complexes presented in this paper shows that the spectroelectrochemical behaviors are not trivial and should help to interpret the behavior of larger supramolecular metallic entities in the future.

Acknowledgment. The authors thank the "Communauté française de Belgique" (ARC 2002-2007, No. 286) for financial support. They are also grateful to the COST D35 program for collaborations and to H. Nierengarten and A. Van Dorsselaer (Université Louis Pasteur, Strasbourg) for the ESMS spectra. L.H. thanks the FRIA (Fonds pour la Recherche dans l'Industrie et l'Agriculture) for a fellowship.

Supporting Information Available: Various spectra of **p-PHEHAT-T**, **T-PHEHAT-p**, **p-TPAC-p**, **T-TPAC-T**, **p-TPAC**, and **T-TPAC**. This material is available free of charge via the Internet at http://pubs.acs.org.

IC070224J